Supplementary Materials

Table S1

Figures S1-S6

Datasets

References

Table S1: Location and record lengths for the 11 charcoal data records from western North America used in this study.

Site ID	Site Name	Lat	Lon.	Record Length (yrs)
7	Foy	48.17	-114.36	13180
8	Bolan	42.02	-123.46	14545
13	Trail	44.28	-110.17	8050
128	Lily Lake	41.98	-120.21	12214
134	Hunters Lake	37.61	-106.84	14260
220	Ruppert	67.07	-154.25	14000
225	7-M	62.50	-113.72	6878
268	Cooley	49.49	-117.65	7551
1077	Lower Gaylor Lake	37.91	-119.29	11679
1129	Todd Lake	44.03	-121.68	7770
1146	Sanger Lake CA	41.90	-123.65	14465

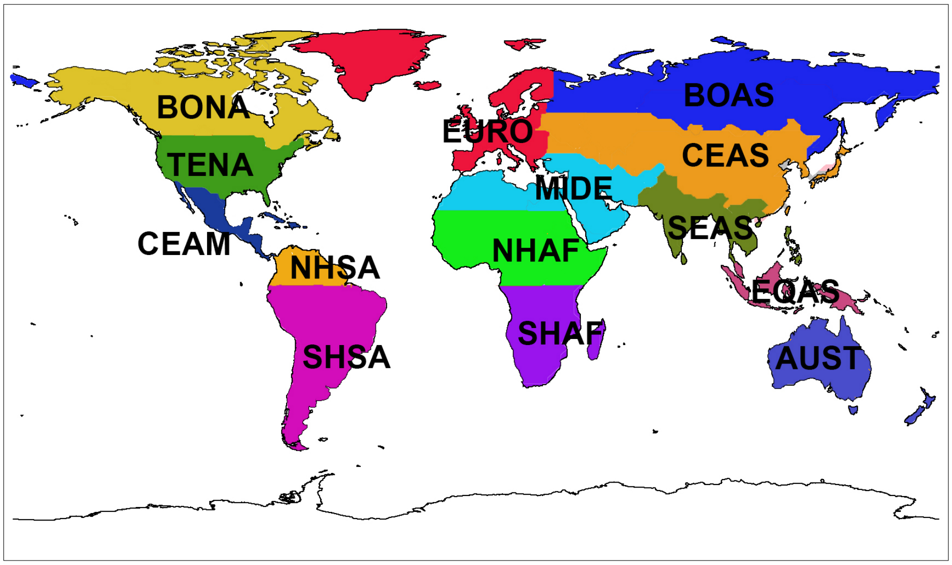

Figure S1: Representation of the regions as defined for the GFED4s and in this study. BONA: Boreal North America, TENA: Temperate North America, CEAM: Central America, NHSA: Northern Hemisphere South America, SHSA: Southern Hemisphere South America, EURO: Europe, MIDE: Middle East, NHAF: Northern Hemisphere Africa, SHAF: Southern Hemisphere Africa, BOAS: Boreal Asia, CEAS: Central Asia, SEAS: Southeast Asia, EQAS: Equatorial Asia, AUST: Australia.

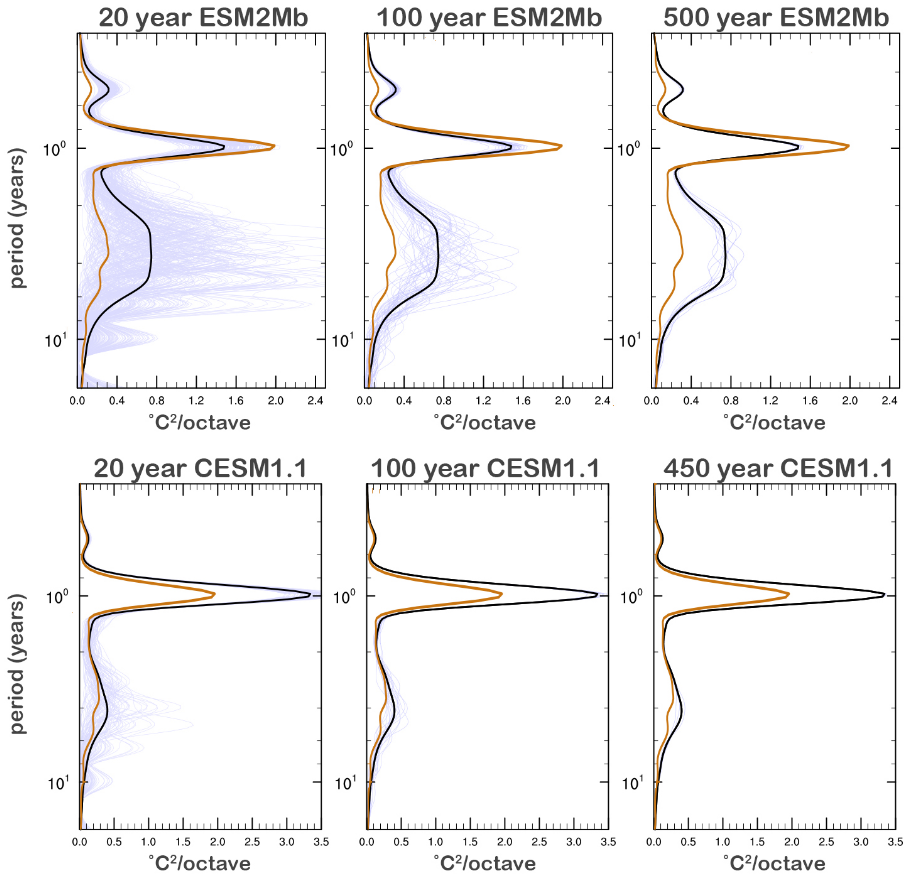

Figure S2: Power spectra of NINO3 SSTs computed using Morlet wavelet analysis with wavenumber-6 with the period expressed as octaves of the annual cycle. Spectra are computed for non-overlapping a) 20-year segments, b) 100-year segments and c) 500-year segments for ESM2Mb and d) 20-year segments, e) 100-year segments, and f) 450-year segments for CESM1. The thick black line gives the average spectrum for the full preindustrial control runs for the respective ESM. The orange line shows the average spectrum for the HadISST1 dataset (Rayner et al., 2003) for 1870 to 2015.

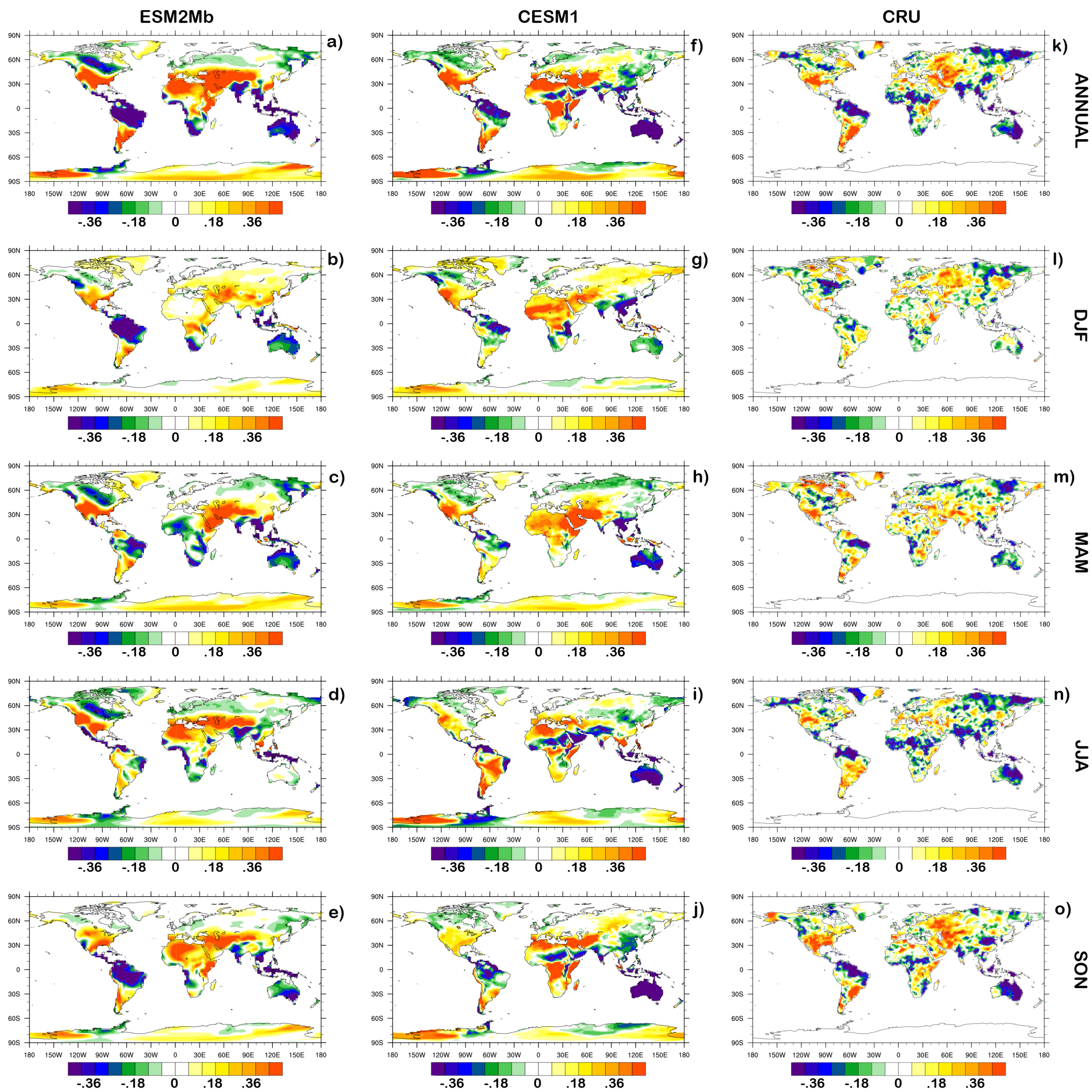

Figure S3: Composite analysis showing differences in the means of standardized anomalies of precipitation for years with positive NINO3 minus years with negative NINO3 for annual precipitation (a: ESM2Mb, f: CESM1.1, k: CRU TS 3.10 [Harris et al., 2014]/HadISST1 [Rayner et al., 2003] 1901-2009), DJF precipitation (b: ESM2Mb, g: CESM1.1, l: CRU TS 3.10/HadISST1), MAM precipitation (c: ESM2Mb, h: CESM1.1, m: CRU TS 3.10/HadISST1), JJA precipitation (d: ESM2Mb, i: CESM1.1, n: CRU TS

3.10/HadISST1), SON precipitation (e: ESM2Mb, j: CESM1.1, o: CRU TS 3.10/HadISST1).

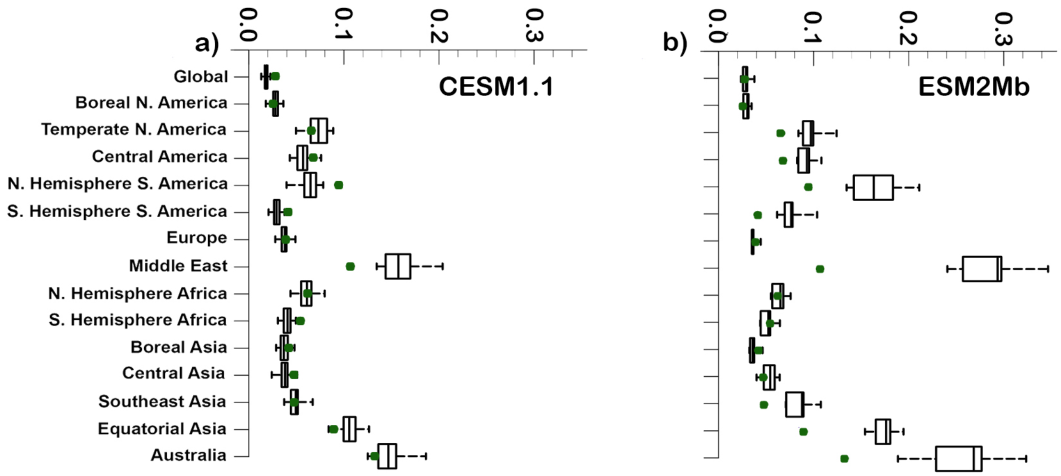

Figure S4: The interannual variability of precipitation from a) CESM1.1 and b) ESM2Mb compared to the CRU TS3.10 (Harris et al., 2014) 1976-2005 precipitation (green circles).

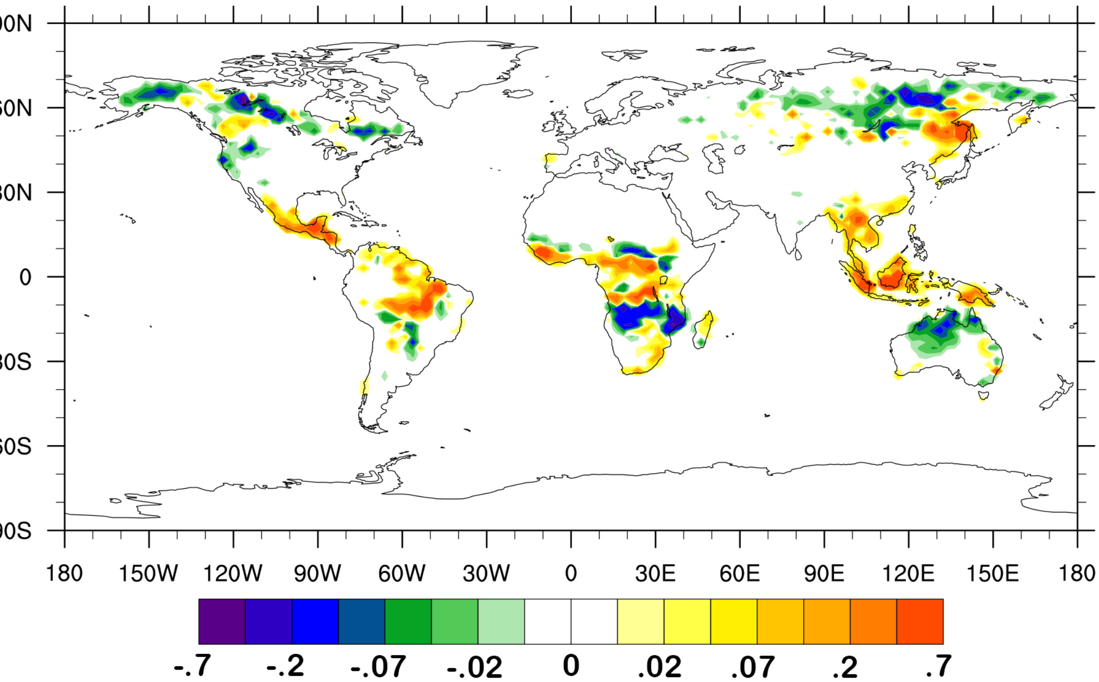

Figure S5: Fire emission anomalies [kgC m^{-2}] from the GFED4s for August 1997 to September 1998 relative to the entire GFED4s record, 1997 to 2014.

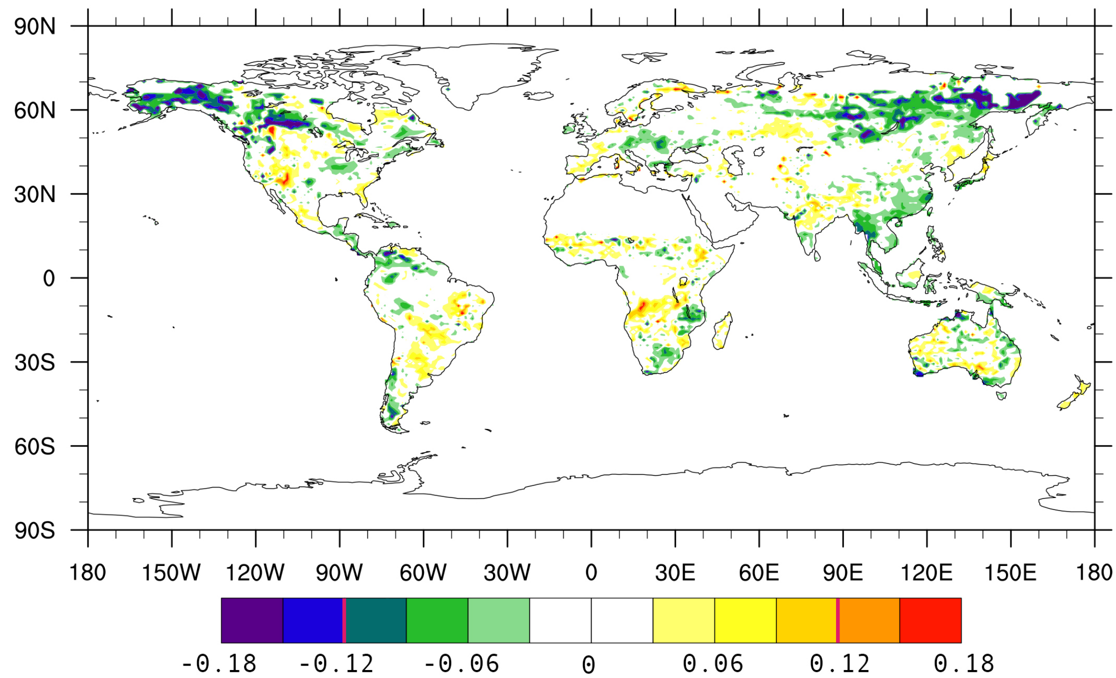

Figure S6: Composite analysis showing differences in the means of standardized anomalies of annual fire emissions for years with positive, 50-year low-pass filtered AMO indices minus years with negative, 50-year low-pass filtered AMO indices from CESM1.1. The values of the difference in means that are significant at a 95% confidence level (two-tailed test) are shown in the colorbars as pink lines.

Datasets

1. GFEDv4s

The Global Fire Emissions Database version 4s (GFED4s) is based on a burned area dataset derived primarily from MODIS (Giglio et al., 2013). Carbon emissions from fires are modeled using the burned area data applied within the Carnegie-Ames-Stanford-Approach (CASA) terrestrial model (Potter et al., 1993; Field et al., 1995; Randerson et al., 1996), which simulates carbon cycling through different pools, including plant litter, and important fire-related processes such as fire-caused vegetation mortality and combustion completeness (Van der Werf et al., 2010). Fires may be consistently underestimated in this inventory in areas with persistent cloud cover that hides active fires from the satellite sensors, and in croplands where fires are often small and escape detection (Van der Werf et al., 2010). An accounting of the emissions from small fires has been made by statistical means (Randerson et al., 2012) and these additional fire emissions are included in the data shown in our study. Fires associated with deforestation and peatlands are isolated from grassland and natural forest fires with ancillary datasets (Giglio et al., 2013).

2. GFASv1

The Global Fire Assimilation System (GFASv1) also uses MODIS to determine global fire activity, but is based on a fire radiative power product instead of burned area (Kaiser et al., 2012). Land-cover dependent conversion factors translate the radiative power into dry-matter combustion rates from which carbon emissions can be derived. The conversion factors are based on theory (Wooster et al., 2005) but scaled to improve the match of the GFAS emissions to GFEDv3 (Kaiser et al., 2012). Compared to GFEDv3, GFASv1 exhibits larger areas of small fire emissions, an aspect that may have been compensated somewhat by the inclusion of small fires in the more recent GFED4s.

3. FINNv1.5

The Fire Inventory from NCAR (FINN) provides higher time (daily) and spatial (~1km) resolution that the previous two inventories (Wiedinmyer et al., 2011), although we re-grid the data to more coarse resolution and use monthly and annual averages for this study. FINN combines active fire counts and land cover data from MODIS to compute total fire emissions from each square kilometer where a fire is detected. Fuel loadings and fraction of vegetation that is burned by fires are derived from MODIS land cover and vegetation type products. In comparison to GFEDv3.1, Wiedinmyer et al. (2011) found that FINN had generally higher emissions from southern hemisphere South America, substantially higher emissions from southeastern Asia, with lower emissions in Africa, Australia and boreal North America. The two inventories report similar global average fire emissions for the period 2005-2009 as examined by Wiedenmyer et al. (2011).

4. Charcoal sediments

Charcoal sediments are often used as a proxy for local and sometimes regional fire emissions and can produce datasets that extend tens of thousands of years into the past (Marlon et al., 2008). Here we make use of data from the Global Charcoal Database (www.paleofire.org) (Power et al., 2008), which is a collection of over 1000 sediment cores taken from six continents. The time resolution of each core, determined by the rate of sedimentation characteristic to the core site, and the period of record vary substantially between sites. Cores with a combination of lengthy record and high time resolution are uncommon. For this study we selected sites with a length of record of at least 4,000 years and time resolution of less than 20 years between timesteps. Western North America had the largest amount of cores that fit these criteria by a large margin (sites listed in Table S2). The data are prepared following the methodology of Marlon et al. (2008) and programming of Blarquez et al. (2014) after linear interpolation to a 20-year timestep. All concentration data are converted to charcoal influx data and undergo Box-Cox transformation and standardization so that different records can be averaged together.

5. Data availability

GFEDv4s: http://www.globalfiredata.org/data.html

GFASv1: http://apps.ecmwf.int/datasets/data/cams-gfas/

FINNv1.5: http://bai.acom.ucar.edu/Data/fire/

GCD: https://www.paleofire.org

CRU TS3.10: http://catalogue.ceda.ac.uk/uuid/3f8944800cc48e1cbc29a5ee12d8542d

HadISST1: http://www.metoffice.gov.uk/hadobs/hadisst/data/download.html

The CESM Large Ensemble Community Project (LENS) has made their ESM output publicly available and interested users are directed to begin at this website: http://www.cesm.ucar.edu/projects/community-projects/LENS/

References

Blarquez O, Vanni`ere B, Marlon J R, Daniau A L, Power M J, Brewer S, Bartlein P J 2014 paleofire: an R package to analyse sedimentary charcoal records from the Global

Charcoal Database to reconstruct past biomass burning *Computers & Geosciences* **72** 255-261.

Field C B, Randerson J T, and Malmstrom C M 1995 Global net primary production – combining ecology and remote sensins *Remote. Sens. Environ* **51** 74–88

Giglio L, Randerson J T, van der Werf G R 2013 Analysis of daily, monthly, and annual burned area using the fourth-generation global fire emissions database (GFED4) *J. Geophys. Res.: Biogeosciences* ***118*** 317–328 doi.org/10.1002/jgrg.20042

Harris I, Jones P D, Osborn T J, Lister D H 2014 Updated high-resolution grids of monthly climatic observations – the CRU TS3.10 Dataset *Int. J. Climatol*. **34** 623–642, doi:10.1002/joc.3711

Kaiser J W, et al. 2012 Biomass burning emissions estimated with a global fire assimilation system based on observed fire radiative power *Biogeosciences* **9** 527–554 doi:10.5194/bg-9-527-2012

Marlon J R, Bartlein P J, Carcaillet C, Gavin D G, Harrison S P, Higuera P E, Joos F, Power M J, Prentice I C 2008 Climate and human influences on global biomass burning over the past two millennia *Nature Geoscience* **1** 697–702 doi.org/10.1038/ngeo313

Potter C S, Randerson J T, Field C B, Matson P A, Vitousek P M, Mooney H A, Klooster S A 1993 Terrestrial ecosystem production - a process model based on global satellite and surface data *Glob. Biogeochem. Cy*. **7** 811–841

Power M J, et al. 2007 Changes in fire regimes since the Last Glacial Maximum: an assessment based on a global synthesis and analysis of charcoal data *Climate Dynamics* **30** 887–907 doi.org/10.1007/s00382-007-0334-x

Randerson J T, Chen Y, van der Werf G R, Rogers B M, Morton D C 2012 Global burned area and biomass burning emissions from small fires *J. Geophys. Res.* **117** G04012 doi.org/10.1029/2012JG002128

Randerson J T, Thompson M V, Malmstrom C M, Field C B, and Fung I Y 1996 Substrate limitations for heterotrophs: Implications for models that estimate the seasonal cycle of atmospheric CO2 *Glob. Biogeochem. Cy.* **10** 585–602

Rayner N A, Parker D E, Horton E B, Folland C K, Alexander L V, Rowell D P, Kent E C, Kaplan A 2003 Global analyses of sea surface temperature, sea ice, and night marine air temperature since the late nineteenth century *J. Geophys. Res*. **108** (D14) 4407 doi:10.1029/2002JD002670

van der Werf G R, Randerson J T, Giglio L, Collatz G J, Mu M, Kasibhatla P S, Morton D C, DeFries R S, Jin Y, van Leeuwen T T 2010 Global fire emissions and the contribution of deforestation, savanna, forest, agricultural, and peat fires (1997– 2009) *Atmos. Chem. Phys*. **10** 11707–11735 doi:10.5194/acp- 10-11707-2010

Wiedinmyer C, Akagi S K, Yokelson R J, Emmons L K, Al-Saadi J A, Orlando J J, Soja A J 2011 The Fire INventory from NCAR (FINN): a high resolution global model to estimate the emissions from open burning *Geosci. Model Dev.* **4** 625–641 doi:10.5194/gmd-4-625-2011

Wooster M J, Roberts G, Perry G L W, Kaufman Y J 2005 Retrieval of biomass combustion rates and totals from fire ra- diative power observations: FRP derivation and calibration relationships between biomass consumption and fire radiative energy release *J. Geophys. Res*. **110** D24311